Published in "Microscopy Research and Technique 71(7): 551 - 556, 2008"
which should be cited to refer to this work.

Angiofil®-Mediated Visualization of the Vascular System by Microcomputed Tomography: A Feasibility Study

SILKE GRABHERR,[1]* ANDREAS HESS,[2] MAREK KAROLCZAK,[3] MICHAEL J. THALI,[1]
SEBASTIAN D. FRIESS,[4] WILLI A. KALENDER,[3] RICHARD DIRNHOFER,[1] AND VALENTIN DJONOV[5]
[1]*Centre of Forensic Imaging, Institute of Forensic Medicine, University of Bern, 3012 Bern, Switzerland*
[2]*Institute of Experimental and Clinical Pharmacology and Toxicology, Friedrich-Alexander-University Erlangen-Nuremberg, 91054 Erlangen, Germany*
[3]*Institute of Medical Physics, Friedrich-Alexander-University Erlangen-Nuremberg, 91052 Erlangen, Germany*
[4]*Gloor Instruments AG, Brauereistr. 10, 8610 Uster, Switzerland*
[5]*Institute of Anatomy, University of Fribourg, 1700 Fribourg, Switzerland*

KEY WORDS Angiofil®; angiogenesis; microangiography; microCT; vascular phenotyping

ABSTRACT Visualization of the vascular systems of organs or of small animals is important for an assessment of basic physiological conditions, especially in studies that involve genetically manipulated mice. For a detailed morphological analysis of the vascular tree, it is necessary to demonstrate the system in its entirety. In this study, we present a new lipophilic contrast agent, Angiofil®, for performing postmortem microangiography by using microcomputed tomography. The new contrast agent was tested in 10 wild-type mice. Imaging of the vascular system revealed vessels down to the caliber of capillaries, and the digital three-dimensional data obtained from the scans allowed for virtual cutting, amplification, and scaling without destroying the sample. By use of computer software, parameters such as vessel length and caliber could be quantified and remapped by color coding onto the surface of the vascular system. The liquid Angiofil® is easy to handle and highly radio-opaque. Because of its lipophilic abilities, it is retained intravascularly, hence it facilitates virtual vessel segmentation, and yields an enduring signal which is advantageous during repetitive investigations, or if samples need to be transported from the site of preparation to the place of actual analysis, respectively. These characteristics make Angiofil® a promising novel contrast agent; when combined with microcomputed tomography, it has the potential to turn into a powerful method for rapid vascular phenotyping.

INTRODUCTION

Microangiography is an important tool for studying the morphology of vessels down to the caliber of capillaries. Studies of this kind are of great biological relevance, since the vascular architecture of tissues and organs reflects their physiological and metabolic properties. Filling vessels with radio-opaque materials is an established procedure and many different compounds have been reported so far (Speck, 2003). Besides the well-known lyophilic salts, mostly barium sulfate, iodized compounds have been historically used, since iodine gives a high radiocontrast.

As an alternative to classical radio-opaque liquids or emulsions, casting techniques are used (Gannon and Hayat, 1978; Murakami, 1971; Nopanitaya et al., 1979). There, blood vessels are filled with resins, e.g., methyl methacrylate, that polymerize within a given timeframe. Upon removal of the biological tissue, a rigid 3D framework is obtained that can be subsequently imaged by conventional microCT, synchrotron-based CT, or confocal microscopy. Interestingly, high-resolution imaging of casted structures has also been achieved with scanning electron microscopy (SEM) (Djonov and Burri, 2004; Hodde and Nowell, 1980; Konerding, 1991; Konerding et al., 1995; Lametschwandtner et al., 1990), although the latter reproduces casts only in two dimensions. New polyurethane-based materials for vascular corrosion casting were recently introduced (Krucker et al., 2006), whereas the more established methacrylate-based systems are on the market for quite some years. Mueller and coworkers have reported on "hierarchical microimaging" (Heinzer et al., 2006), and their article summarizes well the efforts in the field of casting agents.

In practice, radiological microangiography (Barcley, 1947; Rubin, 1964) has permitted the visualization of the microvascular systems of different organs (Barclay and Bentley, 1949; Chang and Trembly, 1961) or venous flaps (Imanishi et al., 1996), and a study on angiogenesis has recently been presented (Djonov and Makanya, 2005). The same methodology has also been applied to investigate the vascular systems of entire small organisms such as mice (Suo et al., 2007) or embryonic chicken (Stoeter et al., 1980). With the former,

*Correspondence to: Silke Grabherr, Institute of Forensic Medicine, University of Lausanne, Rue du Bugnon 21, 1005 Lausanne, Switzerland.
E-mail: silke.grabherr@chuv.ch

Received 31 August 2007; accepted in revised form 28 January 2008

Contract grant sponsor: Virtopsy Foundation, Bern (Switzerland); Contract grant sponsor: DFG; Contract grant number: FG 661 TP4; Contract grant sponsor: BMBF BCCN Physiologie und Bildgebung TP1; Contract grant number: 01GQ0731; Contract grant sponsor: Swiss National Science Foundation; Contract grant number: 3100A0-116243/1.

differences in the vascular systems of wild-type and genetically manipulated mice were evaluated (Folkman, 1996).

We believe that the most promising imaging technique for viewing blood vessels in practice is microcomputed tomography, since it delivers true 3D information and the corresponding data are digitally available for further processing. It is beyond the scope of the present report to summarize all the efforts and developments that have been made in the field of microCT to date. Nevertheless, the most important landmarks for practical work should be seen in the introduction of commercial desktop microCT scanners (Rueegsegger et al., 1996; Sasov and van Dyck, 1997), and—more oriented to basic research—in microtomography by using synchrotron radiation (Bonse and Busch, 1996; Margaritondo, 1988). For a good overview on basic literature dealing with microCT, see Engelke et al. (1999), and for selected original publications, see among others (Flannery et al., 1987; Hoddard et al., 1994). Because microCT is nondestructive, the specimen can be used for further experiments, e.g., it can be subjected to histology after the measurements to gain complementary information (Mueller et al., 2006).

The great benefits that are gained from an analysis of vascular systems by microCT have already been demonstrated (Jorgensen et al., 1998; Karau et al., 2001; Toyota et al., 2002). Various contrast agents have been applied to enhance the vascular signals, and Henkelman and coworkers have described putative advantages and disadvantages for many of them (Marxen et al., 2004). For postmortem angiography, our own group has recently compared and reviewed several methods and compounds (Grabherr et al., 2007). The main problems encountered, especially with particle-based contrast agents, are incomplete mixing, sedimentation, and extravasation. The aim of this feasibility study was, therefore, to evaluate our in-house developed contrast agent Angiofil® for its performance in the visualization of blood vessels in mice postmortem. As we report here, the present method is straightforward and easy to use for accurately screening the vascular system of rodents, e.g., knock-out mice, and largely circumvents the inherent disadvantages of particle-based contrast agents.

MATERIALS AND METHODS

Angiofil®

Angiofil® has recently been developed at the Institute of Forensic Medicine in Bern, and its optimum composition is the subject of ongoing research. It mainly consists of an iodized oil (alkylesters of fatty acids) and a diluting alkane. The ratio of the two components can be adjusted to modify the viscosity of the final liquid. In our experiments, the iodized oil and the diluent were combined at a ratio of 1:5, yielding a viscosity of 3.4 mPa/s at 20°C. In comparison, the viscosity of blood is 4.3 mPa/s and the viscosity of water is 1 mPa/s (both at 21°C), respectively.

Preparation of Samples

Ten 28- to 32-week old wild-type mice (Institute of Experimental and Clinical Pharmacology and Toxicology, Friedrich-Alexander-University Erlangen-Nuremberg, Germany) were used for this study. The animals were housed and cared according to the guidelines of the National Institute of Health. Anesthesia was induced and maintained by an intraperitoneal injection of ketamine (80–100 mg/kg of body weight) and xylazine (10 mg/kg of body weight). Angiofil® was injected manually into the deeply anesthetized mice at room temperature according to two different protocols (see later).

Protocol 1. In the first group of mice ($n = 5$), the abdominal cavity was dissected to visually control the injection and to permit the outflow of blood from the vascular system as it was replaced by the contrast agent. A cannula (0.8 mm × 25 mm, BD Venflon) was inserted into either the right saphenous vein or the inferior vena cava as a route of injection. Angiofil® was then injected manually under visual control until the vascular system was cleared of blood, i.e., until the fluid leaving the vessels of the abdominal wall became colorless. During the manual injection, the heart of the anesthetized animal ceased to beat, typically in less than 2 min.

Protocol 2. In the second group of mice ($n = 5$), the thoracic cavity was dissected and a cannula (0.4 mm × 19 mm) was inserted into the left ventricle of the slowly beating heart. One of the lobes of the liver was opened to break the blood circuit. Initially, a 0.9% solution of sodium chloride was injected into the vascular system to clear it of from blood. Each animal was then perfused either with 4% paraformaldehyde or with acetone to chemically fix the tissue. Acampsia of the tail and the hind limbs indicated that the tissue had been sufficiently well fixed. Angiofil® was then injected under visual control. Upon complete perfusion, the main afferent and efferent vessels of the heart, the liver, the lung, and the kidneys were ligated, and the organs were removed. The individual lobes of the liver and the lung were removed separately. Upon dissection, each organ or part of an organ was placed in a Petri dish and immersed in 4% paraformaldehyde.

MicroCT Imaging and Data Processing

Protocol 1 (Mice 1–5). After removing the cannula, each animal was placed on the table of an in vivo microCT scanner (Tomoscope 30s, VAMP GmbH, Erlangen, Germany). The body of the mouse was scanned in two parts (head to liver and liver to pelvis, respectively) using a tube voltage of 40 kV, a voxel diameter of 40 μm, an acquisition time of 3 min, and a radiation dose of 150 mGy.

Protocol 2 (Mice 6–10). The Petri dishes containing the paraformaldehyde-immersed organs were placed on a microCT scanner (high resolution "ForBild" scanner, Institute of Medical Physics, FAU Erlangen-Nuremberg, Erlangen, Germany). Images were obtained using a tube voltage of 40 kV, a voxel diameter of 15 μm, and an acquisition time of about 1 h. Some of the samples were scanned using a voxel diameter of 10 μm to further improve the resolution of the images.

The obtained scans according to the two protocols were processed using a CT-workstation (Leonardo, Siemens Erlangen, Germany). Both 2D and 3D reconstructions were used for data evaluation. Merging the

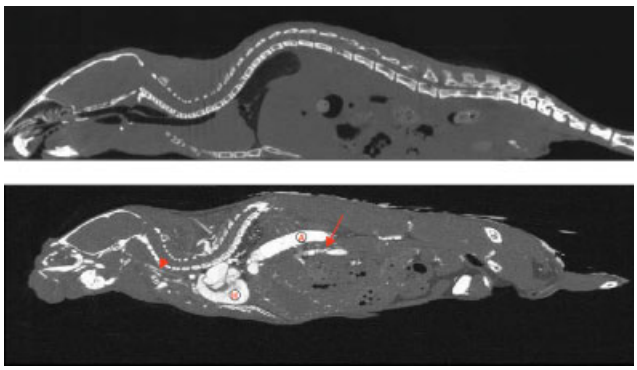

Fig. 1. Reconstructed sagittal cross section images of a mouse. Without addition of a contrast agent (**a**), the heart and the vascular system cannot be distinguished from other soft tissue. Upon injection of Angiofil® into the vascular system (**b**), the heart (H) and the vascular system (A, aorta) become clearly visible. The arrow indicates the mesentery artery and the arrowhead indicates the carotid artery.

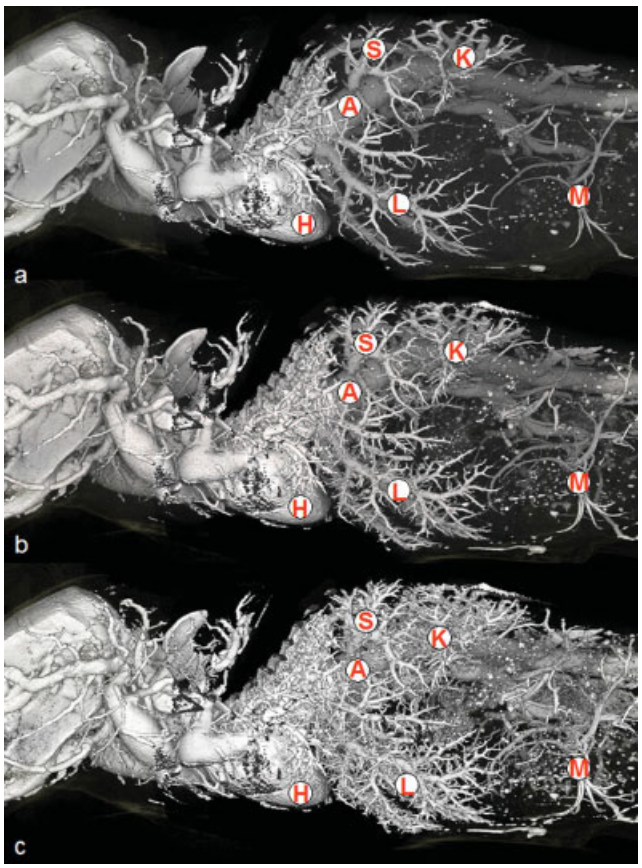

Fig. 2. 3D reconstruction from a microCT scan of a mouse. A part of the skull is visible. The thoracic and abdominal vessels are filled with Angiofil®. The thoracic cage has been virtually removed to facilitate an overview of the vascular system. Letters denominate the thoracic aorta (A) with its branches, the heart (H), vessels of the liver (L), the kidneys (K), the spleen (S), and the mesentery (M). By adjusting the viewing window of the workstation, it is possible to add the visualization of different components of the vascular tree, starting from the main vessels (**a**, top representation), through the medium-sized ones (**b**, middle representation), down to the smallest branches (**c**, bottom representation).

partial body scans of mice 1–5 and building the 3D models were done using the Amira software package (Mercury Computer Systems) or the 3D-reconstruction tools of the CT-workstation. Color coding of vessel caliber and subsequent remapping onto the surface of the 3D model were applied according to our own software code, as previously described (Gaudnek et al., 2005).

RESULTS

To evaluate a novel contrast agent, a straightforward glimpse at contrasted versus uncontrasted sample tissue may be the easiest start. This experiment is readily performed as follows: reconstructed sagittal cross sections of a mouse were obtained without contrast agent (Fig. 1a), and comparatively upon injection of Angiofil® (Fig. 1b). In the latter, the heart and the vascular system are clearly visible, whereas the scans without contrast agent do not show these distinct features.

Mice 1–5 were prepared according to protocol 1, and the corresponding 3D reconstructions of their partial body scans were merged to represent the entire vascular system (Fig. 2). After virtually cutting off the thoracic cage, an overview of the thoracic and abdominal vessels was obtained. Thoracic and abdominal portions of the aorta were demonstrated in their entirety. By adjusting the viewing window on the workstation, the main vessels of the vascular systems of different organs could be visualized according to their caliber size. Vascular branches of the liver could be seen together with their smaller ramifications. Vessels of the spleen and the kidneys, as well as those of the mesentery, were visible as well. The heart was completely filled with the contrast agent, and the cardiac as well as the pulmonary vessels were partially visible. Figure 2a shows the main vessels, whereas Figure 2b comprises also the medium-sized vessels. Figure 2c was reconstructed in an enlarged viewing window which also showed smaller periphery vessels.

Mice 6–10 were prepared according to protocol 2, and high-resolution scans of individual organs revealed the microvessels in great detail (Figs. 3–5). The small arteries and veins, and even the capillaries of the lung (Fig. 3), the kidneys (Fig. 4), and the liver (Fig. 5) were visualized with a spatial resolution down to 15 μm. Remarkable overviews of the main vessels of each organ were obtained. The smallest vessels, such as those of the glomeruli in the kidney, were also visible.

Since individual 2D cross sections were difficult to evaluate (data not shown), maximum intensity projections through all three dimensions were chosen and gave a comprehensive overview of the complete data set. The vascular system was backprojected from maximum intensity images and represented as an "isosurface" (Figs. 3c and 4c) rendered from images above a given threshold. The production of such a surface model is the first segmentation step in the transformation of greyvalue-based images into geometric descriptions of the vascular system. For this purpose, we have used an Amira-based software code (earlier developed in our group, see Gaudnek et al., 2005) that executes each of the steps involved in digital vessel reconstruction.

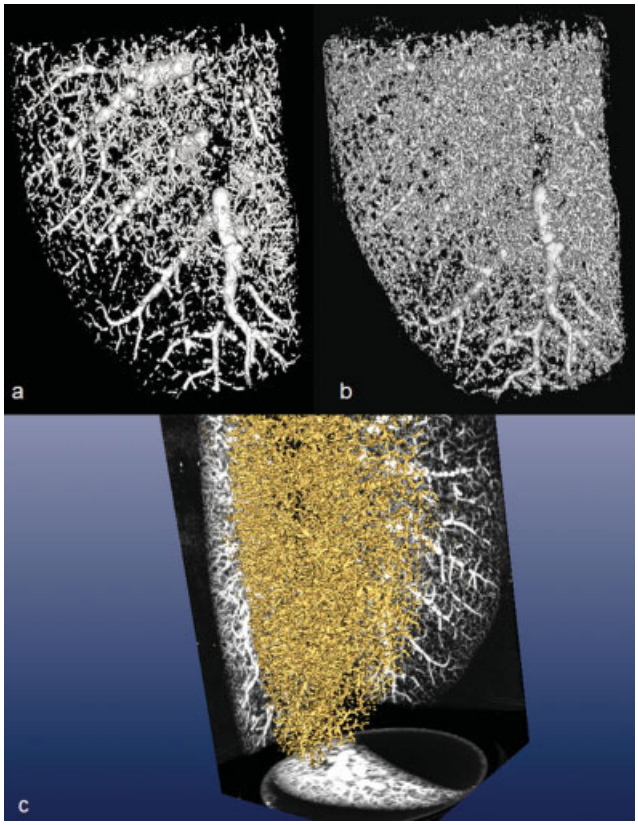

Fig. 3. 3D models of high-resolution scans of a murine lung lobe visualizing the vascular branches (**a**). After adjusting the viewing window, much smaller branches of the vessels become visible (**b**). By using "Amira," the maximum intensity projections on the cube side create an isosurface rendering of the vascular surface (**c**, yellow).

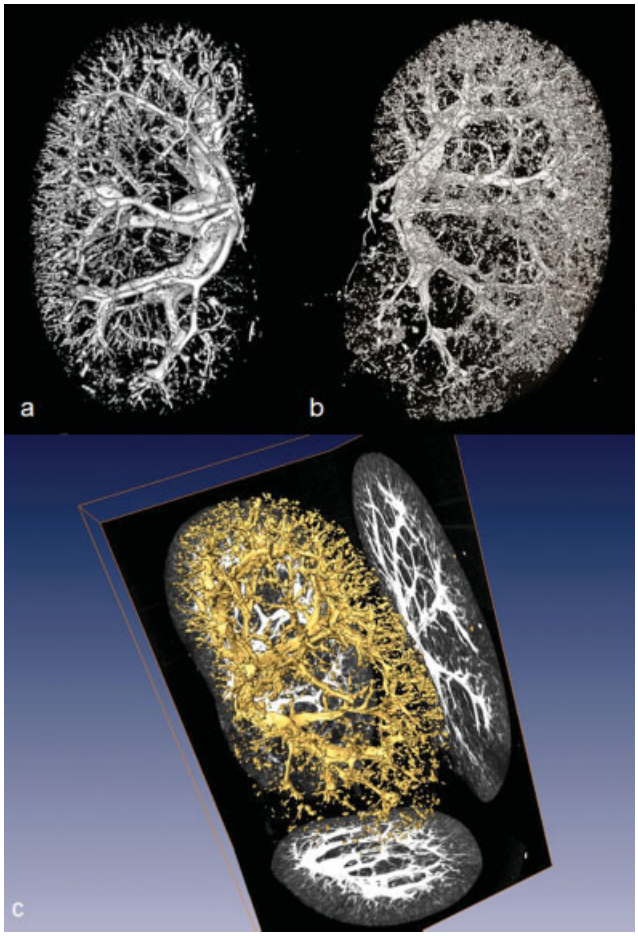

Fig. 4. 3D models of a high-resolution scan of a murine kidney visualizing the interlobular vessels in great detail (**a**). After adjusting the viewing window, the smaller vessels of the cortex and those of the glomeruli become included in the model (**b**). By using "Amira," the maximum intensity projections on the cube side create an isosurface rendering of the vascular surface (**c**, yellow).

For the high-resolution liver scan, vessel calibers were quantified and remapped onto the surface of the vascular system (Fig. 5). In the latter illustration, vessels were color-coded according to their caliber, i.e., from blue via red to yellow, whereas blue represents thinner (light blue: mean diameter up to 50 μm, dark blue: mean diameter 100 μm) and red represents thicker vessels (mean diameter 300 μm), respectively. The thickest parts are marked in yellow (mean diameter 400 μm).

DISCUSSION

Driven by our promising initial results with the above data sets, we are confident that Angiofil® has

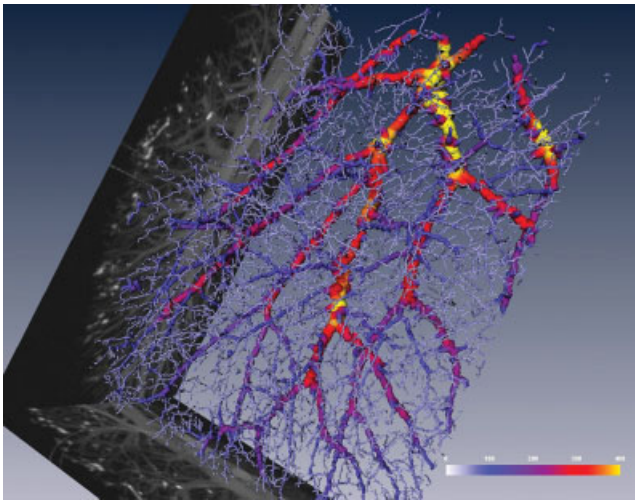

Fig. 5. 3D reconstruction of a high-resolution scan of part of a murine liver, representing the vascular tree with color coding of the vessel caliber (increasing from blue via red to yellow, see color bar, numbers are given in μm). Blue is used for thin vessels (light blue: mean diameter up to 50 μm; dark blue: mean diameter 100 μm) and red is used for thicker vessels (mean diameter 300 μm). The thickest parts are color coded in yellow (mean diameter 400 μm). For the software code of the geometric model see (Gaudnek et al., 2005).

the potential to become a valuable new contrast agent for microangiography. Several points are supporting this as follows:

First of all, Angiofil® is a pure liquid, rather than a particle-based compound. It thus circumvents all the aspects of inhomogeneous mixing, i.e., originated from sedimentation. The latter is known to be one of the most stringent parameters for imaging blood vessels, since incompletely mixed contrast emulsions can eventually lead to virtual disconnection of vessels in the retrieved images (Mueller et al., 2006). A comparison of Angiofil® to more established barium sulfate staining is the subject of ongoing research. Preliminarily, we have found that both contrast agents worked well for lung vessel imaging in rodents; however, the size of the barium sulfate particles strongly influenced infiltration of the vessels, whereas Angiofil® did not show such phenomena (Dominietto et al., in press).

Secondly, Angiofil® is based on an iodized oil which is known to be retained by the vessels for a long time, thus making it well suited for angiography. Pfeifer and Zapata have addressed this issue in detail in macroscopic angiography (Pfeifer et al., 1947; Zapata et al., 1989), and showed that iodized oils were retained in the vessels for at least 72 h before being extravasated. Comparative results were reported by Kan (Kan, 1996), i.e., after injecting an iodized oil into the liver, he observed that it did not penetrate the surrounding tissue. Our own group has carefully monitored the intravascular remaining of oily liquids (Grabherr et al., 2006, 2007) as follows: a probe that has been chemically fixed and filled with an oily contrast agent remains stable for many days without leakage. In this study, we scanned single organs more than 1 week after their perfusion with the contrast agent. No deterioration in image quality was observed. In another study, the time delay between sample preparation and CT analysis was also on the order of several days, without any implications on the experimental results (data not shown). Consequently, organs can be perfused in one laboratory and then sent elsewhere for microCT angiography without the need to rush.

We want to point out that we manually injected the contrast agent into the animals. Organs were perfused manually, too, i.e., without a distinct perfusion control, although at the beginning of our experiments we used a perfusion pump. However, we very soon realized that the effective pressure in the microcirculation depended on many other factors than only perfusion pressure, which was in agreement to earlier findings (Djonov and Burri, 2004). In other words, the pump perfusion pressure was not directly linked to the effective "real" pressure in the vascular tree. We thus abandoned the use of a perfusion pump for this feasibility study.

It is important to note that a user can adapt Angiofil® according to his needs. The viscosity of Angiofil® triggers the degree of embolization, i.e., it directly determines which calibers of the vessels are filled at what degree. Oils with a high viscosity lead to microembolism and to an occlusion of the microcirculation (Grabherr et al., 2006). But when the viscosity is lowered, e.g., by diluting the contrast agent, the oily liquid also penetrates the smaller vessels. In our study, a viscosity of 3.42 mPa/s (at 20°C) was chosen, corresponding to a volumetric 1:5 ratio of Angiofil® versus diluting alkane. As a general recommendation for microangiography, the ratio should be between 1:3 and 1:5, respectively. If only the main vessels, e.g., of a mouse should be visualized, viscosity can be kept high. If the small vessels and capillaries should be investigated, the viscosity can be decreased by adding more diluent. This leads to the possibility of caliber-dependent vessel visualization.

Because of the high radio-opacity of the oily component, injected vessels are sharply contrasted against a signal-free background. This circumstance facilitates the implementation of software solutions for an automated segmentation of the vessel tree and for the calculation of quantitative data, such as vessel length, caliber, and branching geometry. By drawing on the diversity of modern visualization techniques, it is possible to process the digital 3D data obtained from microCT scans in many different ways. Parts of these images can be virtually erased or amplified without destroying the sample. Furthermore, upon scanning, the chemically fixed material is still amenable to a histological analysis.

If an appropriate perfusion technique is employed, then dynamic postmortem angiography becomes feasible (Grabherr et al., 2006). Using a perfusion pump, a postmortem circulation can be established without risk of edemae. Imaging at different time intervals permits a sequential demonstration of different parts of the vascular system, i.e., its arterial, parenchymatous, and venous components.

As a next step, Angiofil® will have to evidence its comparability with respect to established casting methods. We want to point out, that Angiofil® was not developed to replace casting techniques. Cast specimens have several key advantages over classical contrast agents. For example, casts can be subjected to SEM analysis, which eventually allows for final imaging at resolutions down to several nanometers. Nevertheless, casting often fails to maintain the entire vascular network including capillaries, and cast specimens are typically prone to damage during their transport. It should also not be ignored that casting is a time-consuming process that involves a polymerization step. Here, impregnation of individual organs with Angiofil®, or injecting the contrast agent into the animal, may become a straightforward alternative route. To learn more about the comparative performance of Angiofil® versus established casting agents, we have recently started an international research study with several vasculature imaging laboratories.

We have shown that our new contrast agent Angiofil® is able to contrast vasculature without the need of time-consuming sample preparation. A set of 10 mice have served for this microangiography postmortem. Upon microCT scanning, the organs are readily available for further comparative analysis, e.g., histology. With Angiofil®, the user can change the viscosity of the contrast agent and thus trigger a caliber-dependent visualization of the vessels. Since extravasation has not been observed, sample preparation and subsequent analysis can be largely separated in time. By using programs such as "Amira," quantitative analysis of vessel length and caliber is possible; such values can then be color-encoded and remapped onto the surface of the vascular system. We conclude that Angiofil®-mediated

microCT represents a rapid and practicable method for vascular phenotyping.

ACKNOWLEDGMENTS

We thank A. Gaudnek and M. Sibila for their long-lasting cooperation in the processing of images and in the reconstruction of vessels.

REFERENCES

Barclay AE. 1947. Micro-arteriography. Br J Radiol 20:394–404.

Barclay AE, Bentley FH. 1949. The vascularisation of the human stomach. A preliminary note on the shunting effect of trauma. Br J Radiol 22:62–67.

Bonse U, Busch F. 1996. X-ray computed microtomography using synchrotron radiation. Prog Biophys Mol Biol 65:133–169.

Chang CH, Trembly B. 1991. Microangiographic studies of kidney and brain in animals: Technical aspects. Yale J Biol Med 33:451–457.

Djonov V, Burri PH. 2004. Corrosion cast analysis of blood vessels. In: Augustin H, editor. Methods in endothelial cell biology. Berlin Heidelberg: Springer-Verlag. pp. 357–369.

Djonov V, Makanya AN. 2005. New insights into intussusceptive angiogenesis. EXS 94:17–33.

Dominietto M, Friess SD, Grabherr S, Herzen J, Beckmann F, Mueller B. Vessel tree visualization with synchrotron radiation-based micro computed tomography. HASYLAB annual reports, in press. Available at http://hasylab.desy.de/science/annual_reports/hasylab_annual_reports.

Engelke K, Karolczak M, Lutz A, Seibert U, Schaller S, Kalender W. 1999. MicroCT. Technology and application for assessing bone structure (article in German). Radiologe 39:203–212.

Flannery BPH, Deckmann HW, Roberge WG, D'Amico KL. 1987. Three-dimensional X-ray microtomography. Science 237:1439–1444.

Folkman J. 1996. New perspectives in clinical oncology from angiogenesis research. Eur J Cancer A 32:2534–2539.

Gannon BJ, Hayat MA. 1978. Vascular casting. In: Hayat MA, editor. Principles and techniques of scanning electron microscopy. New York: Biol. Applications. pp. 170–193, Chapter 7.

Gaudnek M, Hess A, Obermayer K, Budinsky L, Brune K, Sibila M. 2005. Geometric reconstruction of the RAT vascular system imaged by MRA. ICIP 2:1278–1281.

Grabherr S, Djonov V, Friess A, Thali MJ, Ranner G, Vock P, Dirnhofer R. 2006. Postmortem angiography after vascular perfusion with diesel oil and a lipophilic contrast agent. Am J Roentgenol 187:W515–W523.

Grabherr S, Djonov V, Yen K, Thali MJ, Dirnhofer R. 2007. Postmortem angiography, a review of former and currant methods. Am J Roentenol 188:832–838.

Heinzer S, Krucker T, Stampanoni M, Abela R, Meyer EP, Schuler A, Schneider P, Mueller R. 2006. Hierarchical microimagnig for multiscale analysis of large vascular networks. Neuroimage 32:626–636.

Hoddard WS, McNulty I, Trebes JE, Anderson EH, Lernque RA, Yang L. 1994. Ultrahigh resolution X-ray tomography. Science 2:1213–1215.

Hodde KC, Nowell JA. 1980. SEM of micro-corrosion casts. Scan Electron Microsc (Part 2):89–106.

Imanishi N, Nakajima H, Aiso S. 1996. A radiographic perfusion study of the cephalic venous flap. Plast Reconstr Surg 97:408–412.

Jorgensen SM, Demirkaya O, Ritman EL. 1998. Three-dimensional imaging of vasculature and parenchyma in intact rodent organs with X-ray microCT. Am J Physiol 275:H1103–H1114.

Kan Z. 1996. Dynamic study of iodized oil in the liver and blood supply to hepatic tumors. An experimental investigation in several animal species. Acta Radiol 37(Suppl 408):7–25.

Karau KL, Molthen RC, Dhyani A, Haworth ST, Hanger CC, Roerig DL, Johnson RH, Dawson CA. 2001. Pulmonary arterial morphometry from microfocal X-ray computed tomography. Am J Physiol Heart Circ Physiol 281:H2747–H2756.

Krucker T, Lang A, Meyer EP. 2006. New Polyurethane-based materialfor vascular corrosion casting with improved physical and imaging characteristics. Microsc Res Tech 69:138–147.

Konerding MA. 1991. Scanning electron microscopy of corrosion casting in medicine. Scan Microsc 5:851–865.

Konerding MA, Miodonski AJ, Lametschwandtner A. 1995. Microvascular corrosion casting in the study of tumor vascularity: A review. Scan Microsc 9:1233–1243.

Lametschwandtner A, Lametschwandtner U, Weiger T. 1990. Scanning electron microscopy of vascular corrosion casts—Technique and applications: Updated review. Scan Microsc 4:889–941.

Margaritondo G. 1988. Introduction to synchrotron radiation. New York: Oxford University Press. p. 280.

Marxen M, Thornton MM, Chiarot CB, Klement G, Koprivnikar J, Sled JG, Henkelman RM. 2004. MicroCT scanner performance and considerations for vascular specimen imaging. Med Phys 31:305–313.

Mueller B, Fischer J, Dietz U, Thurner PJ, Beckmann F. 2006. Blood vessel staining in the myocardium for 3D visualization down to the smallest capillaries. Nucl Instrum Methods B 246:254–261.

Murakami T. 1971. Application of the scanning electron microscope to the study of the fine distribution of the blood vessels. Arch Histol Jpn 32:445–454.

Nopanitaya W, Aghajanian JG, Gray LD. 1979. An improved plastic mixture for corrosion casting of the gastrointestinal microvascular system. Scan Electron Microsc 7:751–755.

Pfeifer KJ, Klein U, Chaussy C, Hammer C, Pielsticker K, Haendle H, Lissner J. 1974. Postmortale Nierenvergrößerungsangiographie mit fettlöslichem Kontrastmittel. Fortschr Röntgenstr 121:472–476.

Rubin P. 1964. Microangiography: Facts and artifacts. Radiol Clin North Am 33:499–513.

Rueegsegger P, Koller B, Mueller R. 1996. A microtomographic system for the non-destructive evaluation of bone architecture. Calcif Tissue Int 58:24–29.

Sasov A, van Dyck D. 1997. Desktop X-ray microscopy and microtomography. J Microsc 191(Part 2):151–158.

Speck U. 2003. Kontrastmittel in der Radiologie—Röntgen und MRI. Radiologie up2date 1:81–94. Available at http://www.thieme.com.

Stoeter P, Buchhöcker M, Bruzek W, Drews U, Schulze K. 1980. Angiographic examinations of the circulatory development of living chick embryos. Fortschr Geb Roentgenstr 133:83–91.

Suo J, Ferrara DE, Sorescu D, Guldenberg RE, Taylor WR, Giddens DP. 2007. Hemodynamic shear stresses in mouse aortas: Implications for artherogenesis. Arterioscler Thromb Vasc Biol 27:346–351.

Toyota E, Fujimoto K, Ogasawara Y, Kajita T, Shigeto F, Matsumoto T, Goto M, Kajiya F. 2002. Dynamic changes in three-dimensional architecture and vascular volume of transmural coronary microvasculature between diastolic- and systolic-arrested rat hearts. Circulation 105:621–626.

Zapata MG, Alcaraz M, Luna A. 1989. Study of postmortem blood circulation. Z Rechtsmed 103:27–32.